Nanoscience and Nanometrology
2021; 7(1): 14-26
http://www.sciencepublishinggroup.com/j/nsnm
doi: 10.11648/j.nsnm.20210701.12
ISSN: 2472-3622 (Print); ISSN: 2472-3630 (Online)

An Overview on the Photocatalytic Degradation of Organic Pollutants in the Presence of Cerium Oxide (CeO_2) Based Nanoparticles: A Review

Tigabu Bekele Mekonnen

Department of Chemistry, Mekdela Amba University, Tuluawuliya, Ethiopia

Email address:
tgbekele19@gmail.com

To cite this article:
Tigabu Bekele Mekonnen. An Overview on the Photocatalytic Degradation of Organic Pollutants in the Presence of Cerium Oxide (CeO_2) Based Nanoparticles: A Review. *Nanoscience and Nanometrology*. Vol. 7, No. 1, 2021, pp. 14-26. doi: 10.11648/j.nsnm.20210701.12

Received: January 28, 2021; **Accepted**: March 17, 2021; **Published**: April 20, 2021

Abstract: Considerable efforts have been devoted to enhancing the photocatalytic activity and solar energy utilization of photocatalysts. Photocatalysis has attracted much attention in recent years due to its potential in solving energy and environmental issues. The fabrication of various materials (coupled or doped) to form heterojunctions provides an effective way to better harvest solar energy and to facilitate charge separation and transfer, thus enhancing the photocatalytic activity and stability. Efficient light absorption and charge separation are two of the key factors for the exploration of high performance photocatalytic systems, which is generally difficult to be obtained in a single photocatalyst. In this review, we briefly summarizes the recent development heterostructured semiconductors, including the preparation and performances of semiconductor/semiconductor junctions, semiconductor/metal junctions, and their mechanism in the area of environmental remediation and water splitting for enhanced light harvesting and charge separation/transfer, describe some of the progress and resulting achievements, and discuss the future prospects. The scope of this review covers a variety of type photocatalysts, focusing particularly on Ceria (CeO_2) heterostructured photocatalysts. We expect this review to provide a guideline for readers to gain a clear picture of fabrication and application of different type heterostructured photocatalysts.

Keywords: Nanotechnology, AOPs, Nanoparticle, Ceria, Heterostructure, Photocatalyst, Coupling

1. Introduction

Due to the development of various industries in modern society, water pollution has become one of the most serious environmental problems. Polluted water not only affects the ecological system, causing damages to the livings in water and those relying on the aquatic animals and plants, but also threatens human beings. One of the most common contaminants in wastewater is organic substances, most of which are very stable in natural environment [1]. Hence, they can aggregate in wastewater and are therefore harmful to the aquatic ecosystem. Unfortunately, many industries are producing organic pollutants containing wastewater, which aggravates the water pollution problems [2]. Dye wastes represent one of the most problematic groups of pollutants because they can be easily identified by the human eye and are not easily biodegradable. Generally dyes are very stable to light and oxidation due to the complex aromatic molecular structures, but this causes damage to the environment and dramatically threatens human health [3-5]. Therefore, how to treat wastewater, especially removing organic pollutants in wastewater is one of the most crucial problems for sustainable development [6].

Various conventional treatment methods for dye removal from wastewater include physical, chemical and biological processes such as, anaerobic treatment, trickling filters, flotation, chemical coagulation, electrochemical coagulation, membrane separation, which have been studied so far [7]. However, the main disadvantages of these methods include the production of toxic sludge, high operational cost, technical limitations, lack of effective color reduction and sensitivity to a variable wastewater input. It is also a problem because these dye compounds in wastewater ordinarily contain one or several benzene ring and cannot be decomposed easily in chemical and biological processes. Moreover, most of the dyes are found to be resistant to

normal treatment process.

The use of solar energy and semiconductor catalysts for photocatalytic degradation of organic dyes in water has been intensively investigated as an emerging renewable technology [8-11]. Photocatalysis is one of the advanced oxidation process (AOP) considered as an efficient, stable, and environmentally friendly method in the field of environmental pollution control [12]. It is known that the photocatalysis process can proceed under UV-light or/and visible-light irradiation. Under light irradiation, the organic contaminants can be partially degraded to smaller molecules or even completely mineralized to CO_2 and H_2O [13]. Since visible-light occupies much higher spectral power within solar spectrum than UV-light, visible-light prompted photocatalysis is more advantageous for its efficient utilization of the solar irradiation [14]. Therefore, developing a photocatalyst that can efficaciously degrade organic contaminants under visible-light irradiation is a highly promising direction in the application of wastewater treatment.

Several semiconductor photocatalysts are being used for the treatment of waste water pollutants. Among them TiO_2, ZnO, CeO_2, CdS, Ag_3PO_4 etc... has been reported as a new UV or visible-light-driven photocatalyst for the oxidation of water and photodecomposition of organic compounds [15-19].

Band gap modifications can be carried out by using several approaches such as doping of metal and non-metal elements, metal-metal co-doping, nonmetal-nonmetal co-doping, metal-nonmetal co-doping [20], tri-doping, dye sensitization, deposition of noble metals, and making composite photocatalyst by forming heterojunctions [21-26]. Among the various techniques for the enhancement of visible light effective photocatalysis, composite photocatalysts have drawn more attention owing to their significant increase in photocatalytic activity. Formation of heterojunction between two semiconductors allows the interaction of the band structure which effectively prevents the electron hole recombination thereby enhance the photocatalytic activity [23, 27].

2. Nanostructured Semiconductors

Applying the concept of nanotechnology to heterogeneous catalysis helps us to understand more accurately the transformations occurring on the catalyst´s surface at a molecular level. The synthesis of materials with nanometric dimensions will facilitate a better understanding of the reaction mechanisms as well as to design novel useful catalytic systems. Nanostructured photocatalysts offer large surface to volume ratios allowing higher adsorption of the target molecules. Intensive research over the past decade for its implementation in the purification of drinking water can be found in the literature [28, 29]. Photocatalysis, using nanostructures of metal oxide semiconductors like zinc oxide (ZnO), titania (TiO_2) and ceria (CeO_2) can be an attractive way of water purification as it is capable of removing chemical as well as biological contaminants [30-32]. A good photocatalyst should absorb light efficiently preferably in the visible or near UV part of the electromagnetic spectrum.

2.1. Properties of CeO_2 Nanoparticles

Ceria, which is semiconducting, abundant, nontoxic, and inexpensive, is widely applied in heterogeneous catalytic reactions due to the high mobility of oxygen species and reversible transition between Ce^{4+} and Ce^{3+} oxidation states in CeO_2 crystal. Recent researches have revealed that the size, morphology, surface structure, and synergistic interaction dramatically influence the catalytic performance of CeO_2 [33]. CeO_2 has been shown to be a particularly effective catalyst, in part due to the redox potential of the Ce^{4+}/Ce^{3+} couple, as well as its resistance to chemical and photocorrosion, and strong light absorption in the UV region (absorption edge 385-400 nm). Unfortunately the large band gap (3.2eV) limits further application of CeO_2 [34]. From the AM1.5 spectrum, it can be seen that UV light only composes, 3-5% of the photon flux reaching the earth's surface, while around 45% is in the visible light range. Although photocatalytic activity of CeO_2 has been investigated intensively, the broad band gap energy of this material limits its further application in the visible light region. Hence, efforts have been devoted to improve the light-harvesting capability and photocatalytic activity either by doping or/and coupling with other narrow band gap semiconductors and extend the light absorption of CeO_2 to the visible light region.

2.2. Properties of Ag_3PO_4 Nanoparticles

The development of efficient photocatalysts is very important and desirable in environmental pollution mediation and solar energy conversion.

Among the new materials, silver phosphate (Ag_3PO_4) was reported as a high quantum yield photocatalyst to promote the generation of O_2 in water splitting, because Ag_3PO_4 has appropriate band gap of 2.45 eV for efficient absorption of visible light whose wavelength is shorter than 530 nm [35]. Moreover, the most interesting is that this novel photocatalyst can achieve a quantum efficiency of up to 90% at wavelengths greater than 420 nm, which is significantly higher than the previous reported values. The effects of particle size [36], pH value [37] and morphology [38] of silver phosphate on its photocatalytic activity have also been investigated.

Despite the fact that Ag_3PO_4 is a promising candidate for environmental remediation and renewable energy, the consumption of a large amount of noble metal and the low structural stability of pure Ag_3PO_4 strongly limits its practical environmental applications. Unfortunately, one major limitation of this novel photocatalyst is the instability upon photo-illumination, since it is easily corroded by the photogenerated electrons;

$$(4Ag_3PO_4 + 6H_2O + 12h^+ + 12e^- \rightarrow 12Ag + 4H_3PO_4 + 3O_2)\ [39]\ (1)$$

2.3. Properties of CdS Nanoparticles

Cadmium sulphide (CdS) is a brilliant II-VI semiconductor material with a direct band gap of 2.42 eV at room temperature with many outstanding physical and chemical properties, which has promising applications in multiple technical fields including photochemical catalysis, gas sensor, detectors for laser and infrared, solar cells, nonlinear optical materials, various luminescence devices, optoelectronic devices and so on [40]. Cadmium sulphide (CdS) has excellent visible light detecting properties among the others semiconductors. The photocatalytic activity of CdS is mainly dependent on the electrons and holes which are produced by light absorption.

Photocatalytic process is a photoreaction with a catalyst and depends on the nature of the catalyst because of its ability to create electron-hole pairs, which generate free radicals having the ability to undergo secondary reactions. Preethy et al. reported the synthesis of CdS nanoparticles with photocatalytic activity under visible light. The particle with photoactivity under visible light has wide application in textile and food processing industries [41].

3. Photocatalytic Application of Ceria and Ceria-Based Nanoparticles

Cerium dioxide (CeO_2), as a fascinating rare earth material, has attracted much attention owing to its high activity, low cost and environmentally friendly properties [42, 43]. It shows promising photoactivity for the degradation of organic pollutants and water splitting for hydrogen generation [44]. Nevertheless, pristine CeO_2 can only be excited by ultraviolet light (UV) because of its wide band gap (about 3.2 eV), limiting its further application in the visible light region [45].

In order to highly utilize solar energy, various methods, such as doping, noble metal deposition and forming composites have been designed to enhance the absorption of CeO_2 photocatalysts in the visible light region. Among them, the most effective strategy is the coupling of two semiconductors, CeO_2 and another semiconductor, to form a composite [46-48]. So far, various CeO_2-based composites with a visible light response, such as CdS/CeO_2 [49], CeO_2/Ag_3PO_4 [50], CeO_2/ZnO [51], TiO_2/CeO_2 [52], $TiO_2/CeO_2/ZnO$ [53] and $CdS/CeO_2/Ag_3PO_4$ [54] etc… composite heterostructure appear to be very efficient for the photodecomposition of organic dye than single CeO_2 photocatalysts. The coupled semiconductor with a narrow band gap usually acts as a visible light sensitizer, and the photogenerated electrons or holes excited by visible light irradiation will transfer to the CeO_2. Thus the high efficiency of the interfacial charge transfers as well as the stronger visible light absorption capacity results in the enhanced activity of the composite photocatalysts [55, 56].

3.1. Photocatalytic Activities of Prestine CeO_2 Nanoparticle

As for pure CeO_2, it has been investigated under UV irradiation concerning water splitting for the generation of hydrogen gas [57] and photodegradation of toluene in the gas phase [58]. Zhai *et al*. and Salker and Borker have recently reported the photocatalytic behaviors of CeO_2 under sunlight irradiation to degrade dyes [59, 60]. Herein, we report CeO_2 for photocatalytic degradation of sulfo group-containing azo dyes in aqueous suspension irradiated by visible light. Different azo dye was chosen as model target to examine the adsorption and degradation of azo dye on CeO_2 irradiated by visible light. The CeO_2 showed high photoactivity towards degradation of azo dye and has been proven to be a promising alternative for dye containing wastewater treatment under visible light irradiation.

Ji *et al*. reported the photodegradation of AO7 by aqueous CeO_2 dispersion under visible light illumination at wavelengths longer than 420 nm [43]. The data displayed in Figure 1A clearly indicates that the photocatalytic activity of CeO_2 to degrade azo dye acid orange 7 (AO7) was found to have better performance than commercial reference P25. The temporal UV/Vis spectra showed that the AO7 characteristic band centered at 485 nm decreased promptly upon light irradiation (Figure 1B), indicating that at least the chromophore structure of the dye was destroyed. Peaks at 310 and 228 nm corresponding to naphthalene ring and benzene ring in the dye molecule were also reduced partly, showing a variety of organic molecules present in the solution even after the dispersion is totally bleached [28].

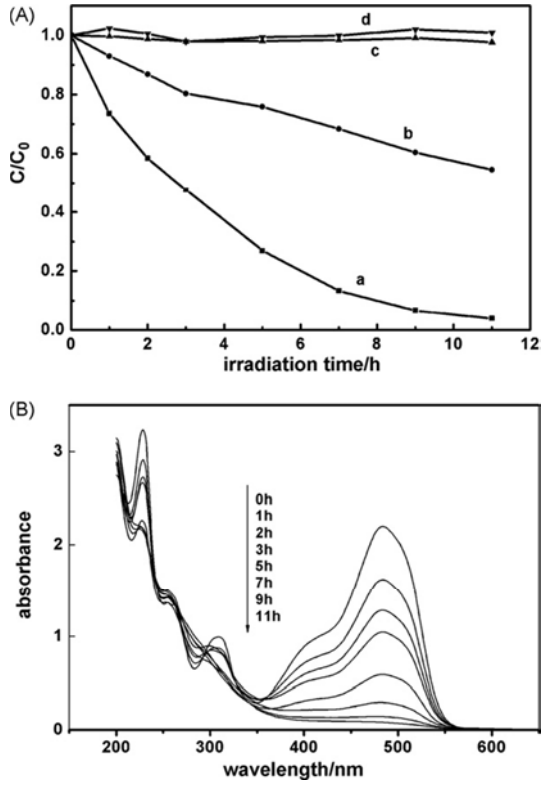

Figure 1. *(A) Temporal course of the photodegradation of AO7 in CeO_2 aqueous dispersions under visible light irradiation: (a) CeO_2 under visible irradiation ($\lambda > 420$ nm). (b) TiO_2 under irradiation ($\lambda > 420$ nm). (c) No catalyst. (d) CeO_2 in the dark. (B) UV/Vis spectral changes recorded for (a) as a function of irradiation time.*

3.2. Photocatalytic Activities of CeO_2/Ag_3PO_4 Nanoparticle

Ag_3PO_4 is a p-type semiconductor with indirect and direct band gaps are 2.36 eV and 2.43 eV, respectively [61]. On account of that the combination of CeO_2 and Ag_3PO_4 possess well matched overlapping band structure [62], p-n hetero-junctions could be fabricated by coupling CeO_2 with Ag_3PO_4, which will bring more effective interface transfer of photo-generated electrons and holes to restrain the recombination. Besides, owe to its narrower band gap relative to CeO_2, Ag_3PO_4 is able to act as efficient photosensitizer to enlarge the light response range under solar light irradiation.

For example Zhang *et al*. studied the photocatalytic activities of Ag_3PO_4/CeO_2 by using Rhodamine B (RhB) as a model pollutant under visible light irradiation [63]. It can be seen that 88.0% of the RhB is photocatalitcally degraded after 60 min irradiation for the Ag_3PO_4/CeO_2 composite. As shown in Figure 2, the photocatalytic activity of the Ag_3PO_4 and CeO_2 sample for RhB degradation is much lower than that of the Ag_3PO_4/CeO_2 p-n heterojunctions. For the pure Ag_3PO_4 and CeO_2 samples, the RhB is degraded by only 47.0% and 10%, respectively. The absorption spectra of RhB (Figure 2a), with 0.1 g of the CeO_2/Ag_3PO_4 p-n heterojunction photocatalyst under visible light irradiation, clearly show that the characteristic absorption peaks corresponding to RhB decrease rapidly as the exposure time increases, indicating the decomposition of RhB and the significant reduction in the RhB concentration.

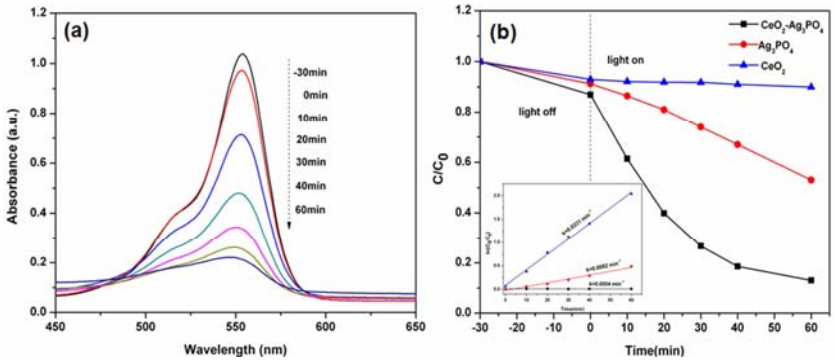

Figure 2. *UV-Vis absorbance spectra of RhB solution after photocatalytic degradation with CeO_2/Ag_3PO_4 heterojunction (a) and RhB concentration C_t/C_0 and $ln(C_0/C_t)$ (inset) vs. time with CeO_2, Ag_3PO_4 and CeO_2/Ag_3PO_4 (b) under visible light irradiation.*

In addition, Song *et al*. found that the pure CeO_2 hardly shows photocatalytic activity under the visible light illumination for MB [50]. After 18 min of the visible-light irradiation, the pure Ag_3PO_4 shows good photocatalytic performance, and its photocatalytic degradation efficiency of MB is about 76%. The CeO_2/Ag_3PO_4 (1 wt. %) composite degrades relatively high level of MB (88%), which is increased by 12% in comparison with the pure Ag_3PO_4. As Ag_3PO_4 is combined with CeO_2, the photocatalytic activity has some improvement, which illustrates that the introduction of CeO_2 is an effective method for the enhancement of photocatalytic performance of the pure Ag_3PO_4. The improvement of photocatalytic activity for CeO_2/Ag_3PO_4 hybrid materials could be attributed to the heterojunction between CeO_2 and Ag_3PO_4.

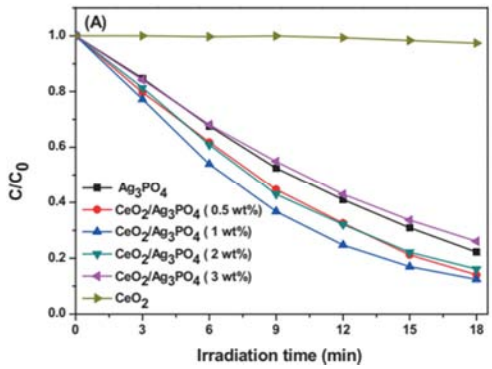

Figure 3. *Degradation of MB under the visible light irradiation with CeO_2/Ag_3PO_4 composites.*

3.3. Photocatalytic Activities of CdS/CeO_2 Nanoparticle

Cadmium sulfide (CdS), a typical II-VI semiconductor, has been extensively studied as visible-light photocatalyst for H_2 evolution and a photosensitizer for sensitizing various wide bandgap metal oxides due to its favorable band-edges more negative than 0 V (vs. NHE), and suitable band-gap (2.4 eV) corresponding well with the spectrum of sunlight. More importantly, CdS can couple well with CeO_2 due to their matched band structures [64, 65]. CdS coupled CeO_2 composite materials have been extensively explored in the field of photocatalysis due to its reinforced visible light absorption capacity and microstructure-dependent photocatalytic properties [66]. Tong and co-workers investigated the photocatalytic performance of CdS/CeO_x nanowires and CdS/CeO_2 nanospheres prepared by electrochemical process, and found that the both composites exhibited hydrogen evolution rate of 223 and 473.6 $\mu molh^{-1}g^{-1}$, respectively, higher than that of pure CeO_2 under visible light illumination.

Gu *et al*. synthesized CdS/CeO_2 nanoparticles and compare the photocatalytic degradation of sample dye Rhodamine B (RhB) under the identical conditions [67]. The results of RhB degradation over CdS, CeO_2 and CdS/CeO_2 photocatalysts were shown in Figure 4. It was noticeable that direct visible light irradiation of the RhB dye solution in the absence of catalysts was inconsequential toward degrading the dye. The maximum degradation efficiency reached to

96.68% after 48 min for the sample. As expected, all samples showed higher photoactivity for the RhB degradation than that of pure CdS and CeO_2 ($\lambda \geq 420$ nm).

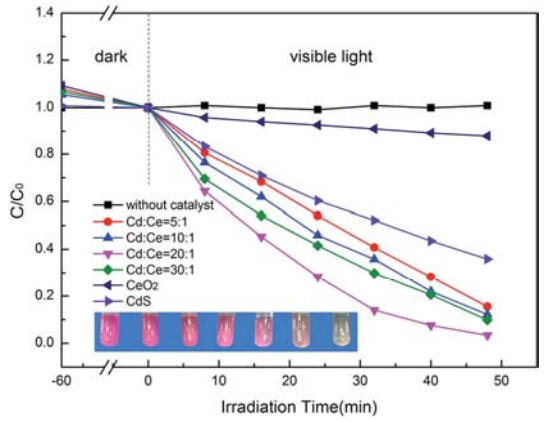

Figure 4. *Effect of CeO_2 loading on photocatalytic degradation of RhB; the suspensions containing 0.4 g/L catalysts, natural pH=4.3, initial concentration=40 mg/L, $\lambda \geq 420$ nm.*

The excellent photocatalytic performances of CdS/CeO_2 heterostructure for RhB degradation may be due to that (i) high oxygen storage capacity of CeO_2 provided immense sources of active species; (ii) the strong interactions between CdS and CeO_2 effectively prevented the photo-corrosion and leaching of CdS; and (iii) effective charge separation reduced the recombination rates of electron-hole pairs [67].

You *et al*. investigated the photocatalytic H_2 production activity of the prepared samples tested under visible light irradiation (> 420 nm) [68]. As shown in Figure 5a and b, the CeO_2 nanoparticles exhibit no activity for H_2 production, which is in accordance with its large bandgap [34]. Coupling with CdS nanoparticle, the CdS/CeO_2 composites exhibit obvious activities for hydrogen evolution, which even higher than that of the bare CdS (1.3 $mmolh^{-1}g^{-1}$). Particularly, the CdS/CeO_2 composite with a mole ratio (1:1) exhibit the highest H_2 evolution rate of 8.4 $mmolh^{-1}g^{-1}$, with a high apparent quantum yield (AQY) up to 11.2%, which is about 6.5 times as high as the CdS nanoparticle. The photocatalytic activities follow the order: CdS/CeO_2 (1:1) > CdS/CeO_2 (2:1) > CdS/CeO_2 (1:2) > CdS/CeO_2 (1:4) > CdS. The as-prepared CdS/CeO_2 (1:1) composite shows higher activity for H_2 evolution and much higher AQY than that of most CeO_2-base composites reported in literatures [69].

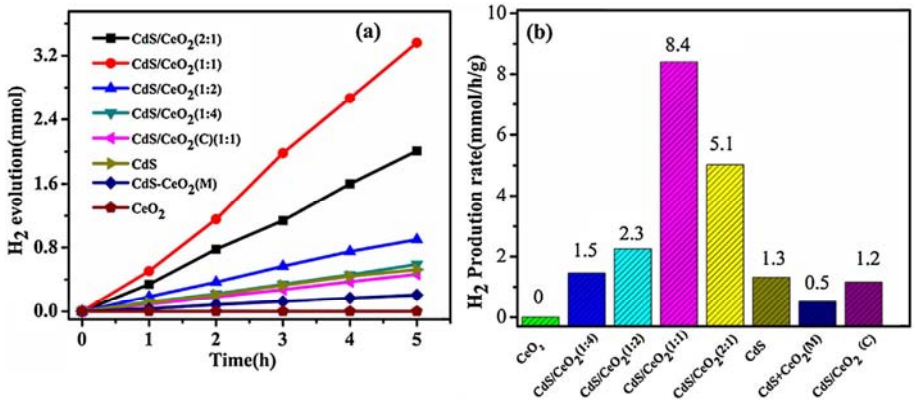

Figure 5. *(a) Time-dependent H_2 production performance, (b) rate of H_2 evolution of bare CdS, CeO_2 and CdS/CeO_2 (n: m) nanocomposites under visible light irradiation.*

3.4. Photocatalytic Activities of CeO_2/TiO_2 Nanoparticles

Recently, rare-earth elements and their oxides have been combined with TiO_2 to improve its photocatalytic activity. Cerium dioxide (CeO_2) is considered to be a suitable candidate to combine with TiO_2 because of its narrow band gap and the Ce^{+4}/Ce^{+3} reversible redox couple [70, 71]. The photocatalytic activities of these composites are obviously enhanced compared with that of TiO_2 or CeO_2 nanoparticles [72].

Chen *et al*. reported the degradation of Rhodamine blue (RhB) dye using CeO_2/TiO_2 nanocomposite [73]. When the CeO_2/TiO_2 nanocomposite was present in the RhB solution, the decrease of intensity of the 554 nm peak was greater than that for the solutions with CeO_2 nanocubes or TiO_2. The absorbance decrease is caused by the cleavage of the conjugated chromophore structure [74], whereas the gradual hypsochromic shift of the absorbance maximum results from stepwise N-deethylation of RhB during irradiation. Degradation of RhB by CeO_2/TiO_2, k is 0.012 min^{-1}, which is still much larger than those of the CeO_2 nanocubes (0.004 min^{-1}) and TiO_2 (0.003 min^{-1}). It is believed that the combination of TiO_2 and CeO_2 in the form of a core shell structure contributes to the improved visible light photocatalytic activity of CeO_2/TiO_2 compared with those of CeO_2 nanocubes and TiO_2.

3.5. ZnO/CeO_2 Nanoparticle to Enhance Photocatalytic Performance

Binary CeO_2/ZnO composites have been reported to be synthesized via various methods, such as atmospheric pressure metal-organic chemical vapor deposition [75], hydrothermal [76], sol-gel method [77] and precipitation technique [78]. The Precipitation method of synthesis is simple, cost-efficient, allows the fabrication of products on a large industrial scale and it provides reproducible results as Nidhi *et al.* reported [79].

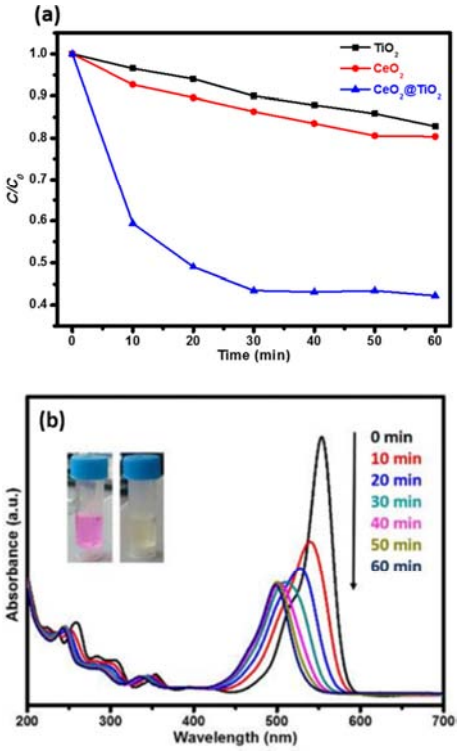

Figure 6. *(a) Photodegradation of RhB with various photocatalyst (b) UV-Vis absorption spectra of solutions of RhB containing CeO_2/TiO_2 nanocomposite under visible light irradiation.*

Nidhi *et al*. compared the photocatalytic activity of CeO_2, ZnO and CeO_2/ZnO core/shell photocatalysts through the degradation of a basic dye Rhodamine B (RhB) in an aqueous solution under UV radiation [79]. Figure 7 depicts the degradation of RhB in the presence of the synthesized core shell composite nanoparticles, under UV radiation at different time. It can be seen that the absorption peaks of RhB solutions gradually decrease along with irradiation time, which indicates that RhB in aqueous solutions is decomposed piece by piece under UV light.

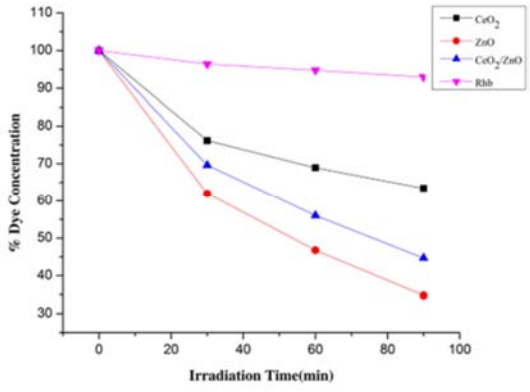

Figure 7. *Degradation of RhB with respect to time in presence of photocatalyst.*

It could be seen that the degradation ratio of Rhodamine B in the presence of nano-sized CeO_2 powder attains 36.56% within 90 minutes of exposure to UV light, while it was 65.20% for RhB in presence of ZnO and 55.33% in presence of composite CeO_2/ZnO nano-sized photocatalyst, respectively, at the same time. Correspondingly, the degradation ratio of RhB in the absence of any catalyst under only UV irradiation was only 7.05% at the same moment. These results indicate that the degradation effects of RhB in the presence of nano-sized catalyst powders are significant than that of unanalyzed system.

The photocatalytic activities of the pristine ZnO and CeO_2/ZnO catalysts were also evaluated in terms of the degradation of methyl orange (MO) under a fluorescent lamp [80]. MO degradation was measured by observing the change in the adsorption spectra of MO at 464 nm, as shown in Figure 8a. Photocatalysts based on CeO_2/ZnO showed higher photocatalytic activity, which can degrade 94.06% of MO after 60 min. In contrast, the photocatalysts based on pristine ZnO can degrade 69.42% of MO. The results suggest an improvement of MO photocatalytic degradation due to an increase in Ce ion doping.

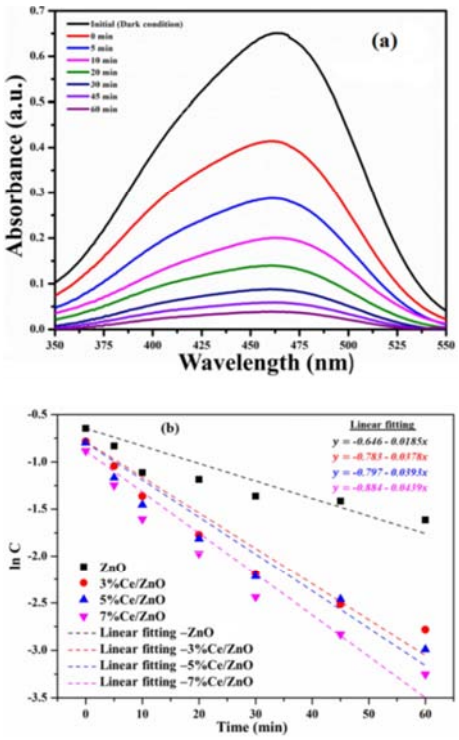

Figure 8. *(a) Change in absorption spectra of the CeO_2/ZnO catalysts (b) First-order kinetic adsorption curves during photodegradation of methyl orange.*

3.6. Photocatalytic Activity of Ceria Based Ternary Nanocomposite

Nanocomposites such as g-C_3N_4/CeO_2/ZnO [81], TiO_2/CeO_2/ZnO [53, 82] $CeO_2/ZrO_2/Al_2O_3$ [83] and $CdS/CeO_2/Ag_3PO_4$ [54] etc… have been considered as effective photocatalysts. The mixing of two different metal oxides leads to not only the thermal stability but also the different physical and chemical property from the individual metal oxides. There are many reports available on mixed metal oxides to improve the thermal stability of Prestine-CeO_2 and increase the photocatalytic activity [84, 85].

3.6.1. g-C_3N_4/CeO_2/ZnO Nanocomposite

Highly efficient g-C_3N_4/CeO_2/ZnO nanocomposite was synthesized by Yuan *et al*. through pyrolysis and subsequent exfoliation method [81]. To study the synergistic effect of the novel g-C_3N_4/CeO_2/ZnO ternary photocatalytic system, the photocatalytic activities of different photocatalysts materials are evaluated for the degradation of methyl blue (MB) solution as a model organic pollutant under irradiation with visible light. Dark adsorption of dye molecules is measured for 20 min to reach an adsorption-desorption equilibrium. In their work, MB, with a characteristic absorption at 663 nm, is chosen as a typical organic pollutant for testing the photocatalytic activity of the as-prepared products under both UV and visible light irradiation.

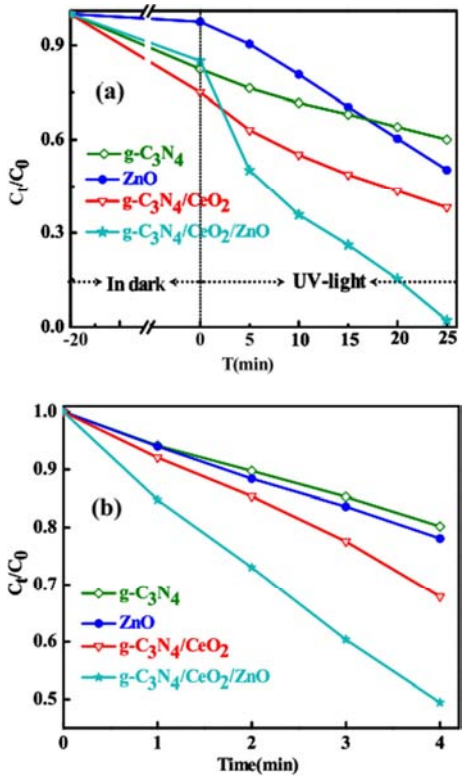

Figure 9. *The photocatalytic activity of the as-synthesized photocatalysts under (a) UV light and (b) Visible light.*

The sag curves in the first 20 min before light irradiation are caused by the MB adsorption-desorption process on the catalyst surfaces. Yuan *et al*. seen that only slight decrease (about 3%) in the concentration of MB can be observed in the presence of ZnO as the adsorption-desorption equilibrium of MB on the surface of ZnO nanoparticles reaches in dark after 20 min ultrasonic treatment [81]. Whereas, the adsorption ability of MB over g-C_3N_4, g-C_3N_4/CeO_2 and g-C_3N_4/CeO_2/ZnO is up to 17.6%, 25% and 15%, respectively, which may be attributed to the nanosheets structure with high specific surface area. They can see that about 50.0%, 40.1%, 62.0% and 98.9% MB is decomposed after 25 min UV light irradiation in the presence of ZnO, g-C_3N_4, g-C_3N_4/CeO_2 nanosheets and g-C_3N_4/CeO_2/ZnO ternary nanocomposites, respectively. These results indicate that the formation of g-C_3N_4/CeO_2/ZnO ternary nanocomposites can greatly enhance the photocatalytic properties on the degradation of pollutants under UV-light irradiation.

The g-C_3N_4/CeO_2/ZnO composite shows the highest photodegradation activity on MB molecules, about 52.0% of the MB is photocatalitcally degraded after 4 h irradiation for the g-C_3N_4/CeO_2/ZnO composite as presented in Figure 9b. In contrast, the MB is photodegraded by only 22.0%, 20.0% and 32.0% in the presence of ZnO, pure g-C_3N_4 and g-C_3N_4/CeO_2samples, respectively. The possible reason for the visible light photocatalytic activity of ZnO may be owing to the defects in ZnO and sensitized effect of dye. The results demonstrate that the degradation efficiency of g-C_3N_4/CeO_2/ZnO composite to MB is much higher than those of pure g-C_3N_4, ZnO and g-C_3N_4/CeO_2 nanosheets under visible light irradiation. Therefore, we can conclude that the formation of the g-C_3N_4/CeO_2/ZnO composite structure facilitates the enhanced photocatalytic activity.

3.6.2. Photocatalytic Activity of CeO_2/ZnO/TiO_2 Composite

Prabhu *et al*. discussed the photocatalytic activity of the composites under visible light irradiation by choosing Rhodamine Blue (RhB) as a model substrate [82]. The photocatalytic activity at 0.2 g/L of catalysts amount and 5 mg/L of dye concentration was shown in Figure 10. The photocatalytic activity of the catalysts depends on the TiO_2 phase present in it. On increasing the percentage of rutile phase in the catalyst, the photocatalytic activity was decreased. The catalyst CZT-A-1 shows high photocatalytic activity as it contains high percentage of anatase phase of TiO_2. Even though the band gap of the catalyst can be decreased from 3.13 to 3.01 eV and 3.13 to 2.91 eV by increasing the calcinations temperature and changing the amount of ZnO and CeO_2, the photocatalytic activity cannot be increased because of phase transformation from anatase to rutile. The high calcinations temperature maybe leads to the formation of thermodynamically stable rutile phase in the composite.

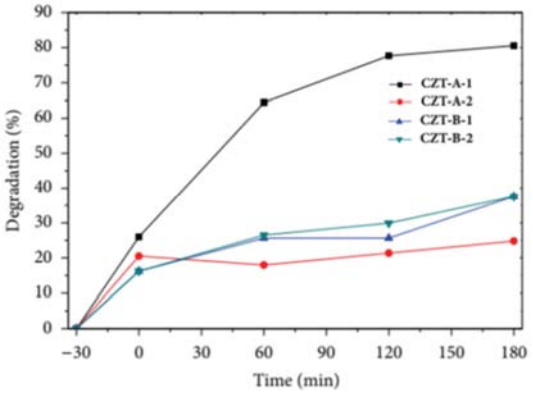

Figure 8. *Degradation of RhB by different photocatalyst load.*

In addition to this Milenova *et al*. compared the performance of the mechanochemically treated TiO_2, CeO_2, ZnO and TiO_2/CeO_2/ZnO photocatalysts in methyl orange (MO) degradation in an aqueous solution [53]. The degrees

of MO degradation line become: TiO_2-MCT (49%) < TiO_2/CeO_2/ZnO-MCT (63%) < CeO_2-MCT (67%) < ZnO-MCT (81%). They assumed that the polar end of MO molecule is irreversibly adsorbed on TiO_2 causing thus deactivation. This can explain the plateau observed in the curve of MO degradation on TiO_2 as indicated in the Figure 11. The nonpolar surfaces of CeO_2 and ZnO exclude such behavior [86].

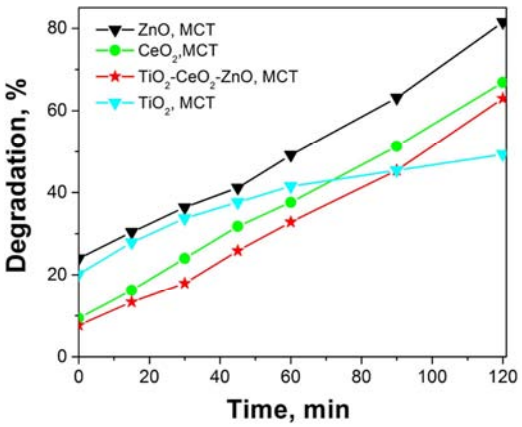

Figure 9. *The degradation of the MO dye in water solution with the course of time under UV-A illumination at 464 nm using TiO_2, CeO_2, ZnO and TiO_2/CeO_2/ZnO photocatalysts.*

3.6.3. Photocatalytic Behavior of Ternary $CdS/CeO_2/Ag_3PO_4$ Photocatalysts

i. Photocatalytic Activity

Abi M. Taddesse *et al*. synthesized ternary $CdS/CeO_2/Ag_3PO_4$ (1:1, 2:1, 3:1 and 4:1 molar ratios) under appropriate conditions [54]. The result exhibited that the highest photocatalytic activity was recorded in case of ternary nanocomposite when compared with both single (CeO_2, CdS and Ag_3PO_4) and binary (CdS/CeO_2 and CeO_2/Ag_3PO_4) congeners see Figure 12a. The reason for the enhancement of ternary nanocomposite is that having more than one path for the formation of electron-hole pair because of the three different interfaces and the delayed electron-hole pair recombination [87, 88].

As shown in Figure 12b, degradation efficiency of bare (CCA1, CCA2, CCA3 and CCA4) and supported ternary nanocomposite over MeO was 52.78, 65.97, 69.77, 81.56 and 90.22% respectively. The photocatalyst comprising polyaniline supported $CdS/CeO_2/Ag_3PO_4$ (PAST) nanocomposite exhibited much higher percentage degradation (90.22%) as compared to the other single, binary and naked ternary counterparts. This could be due to efficient charge separation of electron and hole pairs in the excited states that prevents recombination of charge pairs for a longer time under visible irradiation. Also the conducting polymer PANI has an extended π-conjugated electron system [89], narrow band gap (2.8 eV) semiconductor with high absorption coefficients in the visible light range, and acts as an excellent electron donor and a good hole acceptor when illuminated [90], which makes the PAST highly efficient. These properties make PANI efficient photosensitizer for various semiconductors and provide more active sites for specific binding of dye molecules in order to enhance the separation efficiency of photogenerated electron-hole pairs and consequently better adsorption, photocatalytic activity and stability of the photocatalyst [91, 92].

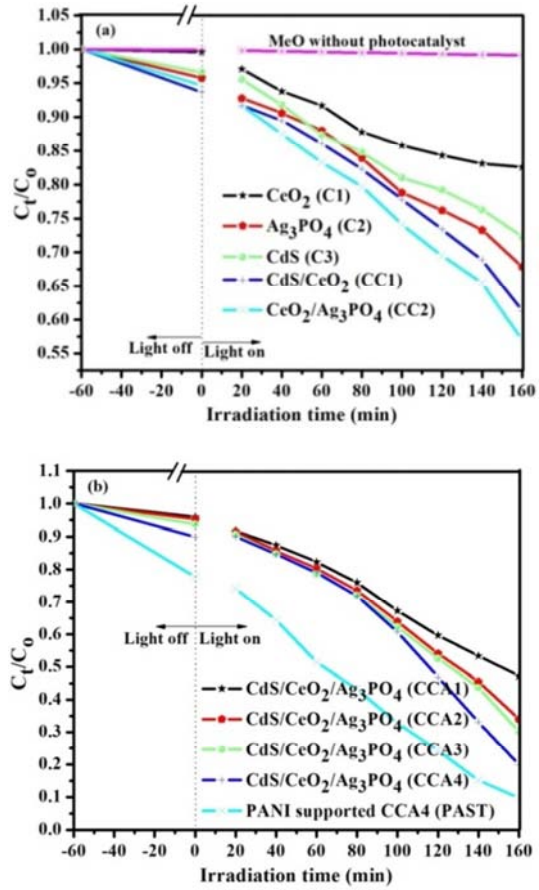

Figure 10. *(a) Degradation efficiency of the as-synthesized photocatalyst [CeO_2, Ag_3PO_4, CdS, CdS/CeO_2 and CeO_2/Ag_3PO_4] as function of visible irradiation time; (b) Photocatalytic degradation of the as-synthesized bare ternary and supported nanocomposite.*

ii. Mechanism of the Photocatalytic Activity of PAST Photocatalyst

A probable mechanism of charge transfer and photocatalytic degradation of organic pollutant methyl orange (MeO) over the polyaniline supported $CdS/CeO_2/Ag_3PO_4$ (PAST) nanocomposite under visible light irradiation is put forward and illustrated in Figure 13 [54]. The light illumination on PAST nanocomposite causes the generation of electron (e^-) in conduction band (CB) and holes (h^+) in the valence band (VB).

Indeed, PANI can absorb visible light to induce the π-π^* transition, delivering the excited state electrons of the highest occupied molecular orbital to the lowest unoccupied molecular orbital [93]. PANI produces e^- that transfers to the CB of $CdS/CeO_2/Ag_3PO_4$ nanocomposite. At CB site, molecular oxygen (O_2) forms superoxide radical $\bullet O_2^-$ in the presence of the photoexcited CB e^- and subsequently reacts with H^+ to form $HO_2\bullet$ radical species. During the e^- transfer

from PANI to CB of CCA4, the generated photoinduced h^+ in VB might react with water (H_2O) and the adsorbed MeO dye molecule to yield hydroxyl radical (•OH) and MeO•$^-$ anions radical respectively [94]. The formed MeO•$^-$ radicals generally transforms to the oxidation and reduction products. On the other hand, electrons in the CCA4 VB can also migrate to the HOMO of PANI and recombine with PANI holes, while the holes generated in the CCA4 VB move to its surface [95]. It is known that these oxygenous radicals ($•O_2^-$, •OH and HO_2•) act as potential oxidizing and reducing species for the degradation of organic molecules (MeO) [96]. The proposed photoreaction mechanism of PAST composite over MeO degradation under visible light follows:

$$PAST + hv \rightarrow h^+_{VB} + e^-_{CB} \quad (2)$$

Oxidative reaction

$$h^+_{VB} + H_2O \rightarrow H^+ + •OH \quad (3)$$

$$•OH + MeO \rightarrow (Intermediates) \rightarrow CO_2 + H_2O$$

Reductive reaction

$$e^-_{CB} + O_2 \rightarrow •O_2^- \quad (4)$$

$$•O_2^- + H^+ \rightarrow •HO_2$$

$$•HO_2 \rightarrow •O_2^- + H_2O_2$$

$$•O_2^- + MeO \rightarrow (Intermediates) \rightarrow CO_2 + H_2O \quad (1)$$

Generally:

$$•O_2^- (•OH, h^+) + MeO + O_2/H_2O \rightarrow \text{Degradation products} \quad (2)$$

The conducting PANI on the surface of CCA4 could absorb photons in the visible light which leads to an efficient photogenerated e^--h^+ pairs charge separation in semiconductors and increases the lifetime of the photogenerated e^--h^+ pairs for diffusing the MeO dye surface. As a result, PAST nanocomposite delivers high photogenerated e^--h^+ pair charge separation and produces sufficiently high amount of radicals for the high degradation of MeO dye under visible light irradiation. The photocatalytic performance of the photocatalyst mainly depends on: (i) its light absorption properties; (ii) the rates of reduction and oxidation on the surface of the catalyst by the electrons and holes; and (iii) the electron-hole recombination rate [97]. These factor results 93.99% of MeO was degraded at optimum pH, initial dye concentration and photocatalyst load under the visible light irradiation.

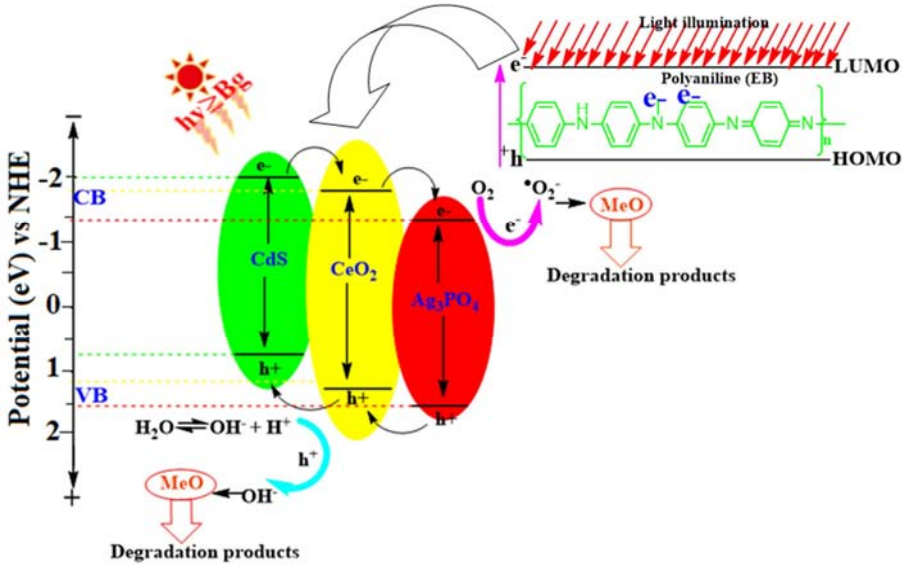

Figure 11. *Mechanism of photocatalytic degradation of organic contaminant (MeO) by PAST photocatalyst under visible light irradiation.*

4. Conclusion and Future Trends

These review was aimed to evaluate the potential of Ceria (CeO_2) based photocatalyst for photocatalytic wastewater treatment. Coupled nanocomposites namely single, binary and ternary were studied. Photocatalytic degradation activities of the nanocomposite under UV or visible light irradiation have been evaluated for different model pollutant. This review demonstrated that coupling is useful to improve the photocatalytic performance of the photocatalysts for degradation of hazardous chemicals. Also it provides a systematic concept about how coupling contribute to improving the performance of composite photocatalysts. Coupled nanostructured CeO_2 have been reported to result in improved degradation rates due to their modified band gap energy for using visible and solar radiation. More studies needs to be carried out in this area to design efficient photocatalytic materials by tuning their band gap to obtain synergistic structure property relationship. Majority of the studies reveals that different supporting materials (either doping or coupling) act as effective sensitizers for CeO_2.

So, we need to focus for developing more reliable photocatalysts which can absorb visible and solar radiation or

by both.

1) The author recommends other researchers to pay attention for advancing further research on this particular area by extending their modification to improve absorption of light.
2) Looking for other polymeric or inorganic supports or organic/inorganic doped to enhance the photocatalytic efficiency.
3) Supporting the photocatalyst by conductive polymers are also possible solving routes to increase the lifetime of the photo-produced electron-hole pairs and improvement of the photocatalytic activity of ceria.
4) Study on the effect of operational parameters such as pH, initial dye concentration, photocatalyst load, light intensity, calcination temperature, and effect of surface area of a photocatalyst on the photocatalytic degradation of organic pollutants.
5) For this a successful collaboration of chemical engineers and chemists is required which would provide better insight and solutions to issues that are hindering commercialization of doping or coupling CeO_2 photocatalysts.

Competing Interests

The author declares that there is no competing interest.

Acknowledgements

Above all, I would like to extend my special thanks to Dr. Abi Taddesse, for his encouragement and genuine support on the knowledge of nanotechnology. I am indebted to the College of Natural and Computational Sciences and Department of Chemistry in Mekdela Amba University for their contributions in the process of developing the review and provision of various services as well as for providing me a great opportunity to advance intellectually.

References

[1] Han, F, Kambala, V. S. R, Srinivasan, M, Rajarathnam, D. and Naidu, R. 2009. Tailored titanium dioxide photocatalysts for the degradation of organic dyes in wastewater treatment: A review. *Applied Catalysis* A, 359: 25-40.

[2] Gogate, P. R. and Pandit, A. B. 2004. A review of imperative technologies for wastewater treatment I: oxidation technologies at ambient conditions. *Advance in environmental research*, 8: 501-551.

[3] Chen, H. and Zhao, J. 2009. Adsorption study for removal of Congo red anionic dye using organo-attapulgite. *Adsorption*, 15 (4): 381-389.

[4] Ong, S. T., Keng, P. S., Lee, W. N., Ha, S. T. and Hung, Y. T. 2011. Dye waste water treatment. *Water review* 3: 157-176.

[5] Huo, S. H. and Yan, X. P. 2012. Metal-organic framework MIL-100 (Fe) for the adsorption of malachite green from aqueous solution. *Journal of Materials Chemistry*, 22: 7449-7455.

[6] Brown, M. A. and De Vito, S. C. 1993. Predicting azo dye toxicity. *Critical Reviews in Environmental Science and Technology*, 23: 249-324.

[7] Kornaros, M. and Lyberatos, G. 2006. Biological treatment of wastewaters from a dye manufacturing company using a trickling filter. *Journal of Hazardous Material*, 136: 95 102.

[8] Chen, C., Ma, W. and Zhao, J. 2010. Semiconductor-mediated photodegradation of pollutants under visible-light irradiation. *Chemical Society Reviews*, 39 (11): 4206-4219.

[9] Kubacka, A., Fernandez-Garcia, M. and Colon, G. 2011. Advanced nano-architectures for solar photocatalytic applications. *Chemical Reviews*, 112 (3): 1555-1614.

[10] Dolbecq, A., Mialane, P., Keita, B. and Nadjo, L. 2012. Polyoxometalate-based materials for efficient solar and visible light harvesting: application to the photocatalytic degradation of azo dyes. *Journal of Materials Chemistry*, 22 (47): 24509-24521.

[11] Fan, W., Zhang, Q. and Wang, Y. 2013. Semiconductor-based nanocomposites for photocatalytic H_2 production and CO_2 conversion. *Physical Chemistry Chemical Physics*, 15 (8): 2632-2649.

[12] Anandan, S., Vinu, A., Mori, T., Gokulakrishnan, N., Srinivasu, P., Murugesan, V. and Ariga, K. 2007. Photocatalytic degradation of 2, 4, 6-trichlorophenol using lanthanum doped ZnO in aqueous suspension. *Catalysis Communications*, 8 (9): 1377-1382.

[13] Hoffmann, M. R., Martin, S. T., Choi, W. and Bahnemann, D. W. 1995. Environmental applications of semiconductor photocatalysis. *Chemical Reviews*, 95 (1): 69-96.

[14] Asahi, R., Morikawa, T., Ohwaki, T., Aoki, K. and Taga, Y. 2001. Visible-light photocatalysis in Nitrogen-Doped Titanium Oxides. *Science*, 293: 269-271.

[15] Bi, Y., Ouyang, S., Cao, J. and Ye, J. 2011. Facile synthesis of rhombic dodecahedral AgX/Ag_3PO_4 (X=Cl, Br, I) heterocrystals with enhanced photocatalytic properties and stabilities. *Physical Chemistry Chemical Physics*, 13 (21): 10071-10075.

[16] Montini, T., Gombac, V., Hameed, A., Felisari, L., Adami, G. and Fornasiero, P. 2010. Synthesis, characterization and photocatalytic performance of transition metal tungstates. *Chemical Physics Letter*, 498: 113-119.

[17] Bi, Y., Hu, H., Ouyang, S., Lu, G., Cao, J. and Ye, J. 2012. Photocatalytic and photoelectric properties of cubic Ag_3PO_4 sub-microcrystals with sharp corners and edges. *Chemical Communications*, 48 (31): 3748-3750.

[18] Ran, J., Yu, J. G. and Jaroniec, M. 2011. $Ni(OH)_2$ modified CdS nanorods for highly efficient visible-light-driven photocatalytic H_2 generation. *Green Chemistry*, 13: 2708-2713.

[19] Wang. Y., Xiuli., Wan, Y. and Fan, C. 2013. Novel visible-light $AgBr/Ag_3PO_4$ hybrid's photocatalysts with surface plasma resonance effects. *Journal of Solid State Chemistry*, 2002: 51-56.

[20] Wang, H., Zhang, L., Chen, Z., Hu, J., Li, S., Wang, Z., Liu, J. and Wang, X. 2014. Semiconductor heterojunction photocatalysts: design, construction, and photocatalytic performances. *Chemical Society Reviews*, 43: 5234-5244.

[21] Dana, D., Vlasta, B., Mazur, M. and Malati, M. A. 2002. Investigations of metal-doped titanium dioxide photocatalysts. *Applied Catalysis*, 37: 91-105.

[22] Liu, Y., He, L., Mustapha, A., Li, H., Hu, ZQ., Lin, M. 2009. Antibacterial activities of zinc oxide nanoparticles against Escherichia coli. *Journal of Applied Microbiology*, 015 (107): 1193-1201.

[23] Zhang, M., An, T., Liu, X., Hu, X., and Sheng, G. 2010. Rapid large scale preparation of ZnO nanowires for photocatalytic application. *Journal of Nanoscale Research Letters*, 64: 1883-1886.

[24] Tesfay, Wolderufael., O. P., Yadav, and Abi M, Taddesse, 2013. Synthesis, characterization and photocatalytic activity of AgN-codoped ZnO nanoparticles towards methyl red degradation. *Bulletin Chemical Society of Ethiopia*, 27: 221-232.

[25] Alebel, Nibret, O. P., Yadav., Isabel, Diaz, and Abi M, Taddesse, 2015. Cr-N Co-doped ZnO nanoparticles: synthesis, characterization and photocatalytic activity for degradation of Thymol blue. *Bulletin Chemical Society Ethiopia*, 29 (2): 247-258.

[26] Haile Hasana, Abi Tadesse. and Tesfahun Kebede. 2015. Synthesis, characterization and photocatalytic activity of $MnO_2/Al_2O_3/Fe_2O_3$ nanocomposite for degradation of malachite green. African Journal of Pure and Applied Chemistry, 9 (11): 211-222.

[27] Shamaila, S., Sajjad, A. K. L., Chen, F. and Zhang, J. 2011. WO_3/BiOCl a novel heterojunctions visible light photocatalyst. *Journal of colloids and interface Science*, 356: 465-472.

[28] Stylidi, M., Kondarides, D. I. and Verykios, X. E. 2004. Visible light-induced photocatalytic degradation of Acid Orange 7 in aqueous TiO_2 suspensions. *Applied Catalysis* B: *Environmental*, 47 (3): 189-201.

[29] Colmenares, J. C., Aramendia, M. A., Marinas, A., Marinas, J. M. and Urbano. F. J. 2006. Synthesis, characterization and photocatalytic activity of different metal doped Titania systems. *Applied Catalysis*, 306: 120-127.

[30] Curco, D., Gimenez, J., Addardak, A., Cervera-March, S. and Esplugas, S. 2002. Effects of radiation absorption and catalyst concentration on the photocatalytic degradation of pollutants. *Catalysis Today*, 76: 177-188.

[31] Palmisan, G., Addam, M., Augugliar, V., Caronna, T., Di Paola, A., Lopez, E. G., Lodd, V., Marci, G., Palmisan, L. and Schiavell, M. 2007. Selectivity of hydroxyl radical in the partial oxidation of aromatic compounds in heterogeneous photocatalysis. *Catalysis Today*, 122: 118-127.

[32] Wang, S. P., Zhao, L. F., Wang, W., Zhao, Y. J., Zhang, G. L., Ma, X. B. and Gong, J. L. 2013. Morphology control of ceria nanocrystals for catalytic conversion of CO_2 with methanol. *Nanoscale*, 5: 5582-5588.

[33] Sun, C., Li, H. and Chen, L. 2012. Nanostructured ceria-based materials: synthesis, properties, and applications. *Energy and Environmental Science*, 5 (9): 8475-8505.

[34] Magesh, G., Viswanathan, B., Viswanath, R. P. and Varadarajan, T. K. 2009. Photocatalytic behavior of CeO_2-TiO_2 system for the degradation of methylene blue. *Indian Journal of Chemicals*, B. 3: 480-488.

[35] Umezawa, N., Shuxin, O. and Ye, J. 2011. Theoretical study of high photocatalytic performance of Ag_3PO_4. Physical review, B. 83: 035202.

[36] Khan, A., Qamar, M. and Muneer, M. 2012. Synthesis of highly active visible-light-driven colloidal silver orthophosphate. Chemical Physics Letters, 519-520: 54-58.

[37] Ge, M., Zhu, N., Zhao, Y., Li, J. and Liu, L. 2012. Sunlight-assisted degradation of dye pollutants in Ag3PO4 suspension. Industrial and Engineering Chemistry Research, 51 (14): 5167-5173.

[38] Dong, P., Wang, Y., Li, H., Li, H., Ma, X. and Han, L. 2013. Shape-controllable synthesis and morphology-dependent photocatalytic properties of Ag_3PO_4 crystals. Journal of Materials Chemistry. A, Materials for Energy and Sustainability, 1 (15): 4651.

[39] Yi, Z., Ye, J., Kikugawa, N., Kako, T., Ouyang, S. and Williams, S. H. 2010. An orthophosphate semiconductor with photooxidation properties under visible-light irradiation. Nature Materials, 9 (7): 559-564.

[40] Erra, S., Shivakumar, C., Zhao, H., Barri, K., Morel, D. L. and Frekides, C. S. 2007. An effective method of Cd incorporation in CdS solar cells for improved stability. Thin Solid Films, 515: 5833.

[41] Preethy, C., Kumari, P. and Sudheer, S. K. 2014. Photocatalytic activation of CdS NPs under visible light for environmental cleanup and disinfection. Solar Energy, 105: 542-547.

[42] Lu, X., Zhai, T., Cui, H., Shi, J., Xie, S., Huang, Y., Liang, C. and Tong, Y. 2011. Redox cycles promoting photocatalytic hydrogen evolution of CeO_2 nanorods. *Journals of Material Chemistry*, 21 (15): 5569-5572.

[43] Ji, P., Zhang, J., Chen, F. and Anpo, M. 2009. Study of adsorption and degradation of Acid Orange 7 on the surface of CeO_2 under visible light irradiation. *Applied Catalysis* B, 85 (3-4), 148-154.

[44] Primo, A., Marino, T., Corma, A., Molinari, R. and Garcia, H. 2011. Efficient visible-light photocatalytic water splitting by minute amounts of gold supported on Nanoparticulate CeO_2 obtained by a biopolymer Templating method. *Journal of American Chemical Society*, 133 (18): 6930-6933.

[45] Feng, Y. J., Liu, L. L. and Wang, X. D. 2011. Hydrothermal synthesis and automotive exhaust catalytic performance of CeO_2 nanotube arrays. *Journal of Material Chemistry*, 21 (39): 15442-15448.

[46] Hu, S., Zhou, F., Wang, L. and Zhang, J. 2011. Preparation of Cu_2O/CeO_2 heterojunction photocatalyst for the degradation of Acid Orange 7 under visible light irradiation. *Catalysis Communication*, 12 (9): 794-797.

[47] Yue, L. and Zhang, X. M. 2009. Structural characterization and photocatalytic behaviors of doped CeO_2 nanoparticles. *Journal of Alloys Compound*, 475 (1-2): 702-705.

[48] Zhang, J., Li, L., Huang, X. and Li, G. 2012. Fabrication of Ag-CeO_2 core-shell nanospheres with enhanced catalytic performance due to strengthening of the interfacial interactions. *Journal of Material Chemistry*, 22 (21): 10480-10487.

[49] Ijaz, S., Ehsan, M. F., Ashiq, M. N., Karamat, N. and He, T. 2016. Preparation of CdS/CeO_2 core/shell composite for photocatalytic reduction of CO_2 under visible-light irradiation. *Applied Surface Science*, 390: 550-559.

[50] Song, Y., Zhao, H., Chen, Z., Wang, W., Huang, L., Xu, H. and Li, H. 2016. The CeO_2/Ag_3PO_4 photocatalyst with stability and high photocatalytic activity under visible light irradiation. *Physical Status Solidi* A, 213 (9): 2356-2363.

[51] Velusamy, P. and Lakshmi, G. 2017. Enhanced photocatalytic performance of (ZnO/CeO_2)-b- CD system for the effective decolorization of Rhodamine B under UV light irradiation. *Applied Water Science*, 7: 4025-4036.

[52] Saikia, P., Miah, A. T. and Das, P. P. 2017. Highly efficient catalytic reductive degradation of various organic dyes by Au/CeO_2-TiO_2 nano-hybrid. *Journal of Chemical Sciences*, 129 (1): 81-93.

[53] Milenova, K., Zaharieva, K., Stambolova, I., Blaskov, V., Eliyas, A. and Dimitrov. L. 2017. Photocatalytic performance of TiO_2, CeO_2, ZnO and TiO_2-CeO_2-ZnO in the course of methyl orange dye degradation. *Journal of Chemical Technology and Metallurgy*, 52 (1): 13-19.

[54] Abi M. Taddesse., Tigabu Bekele., Isabel Diaz. and Abebaw Adgo. 2021. Polyaniline supported $CdS/CeO_2/Ag_3PO_4$ nanocomposite: An "A-B" type tandem n-n heterojunctions with enhanced photocatalytic activity. *Journal of Photochemistry and Photobiology*, A: *Chemistry*, 406: 113005.

[55] Pouretedal, H. R., Tofangsazi, Z. and Keshavarz, M. H. 2012. Photocatalytic activity of mixture of ZrO_2/SnO_2, ZrO_2/CeO_2 and SnO_2/CeO_2 nanoparticles. *Journal of Alloys Compound*, 513: 359-364.

[56] Yao, W., Zhang, B., Huang, C., Ma, C., Song, X. and Xu, Q. 2012. Synthesis and characterization of high efficiency and stable Ag_3PO_4/TiO_2 visible light photocatalyst for the degradation of methylene blue and Rhodamine B solutions. *Journal of Material Chemistry*, 22 (9): 4050- 4055.

[57] Bamwenda, G. R and Arakawa, H. J. 2000. Cerium dioxide as a photocatalyst for water decomposition to O_2 in the presence of Ce^{4+} aq and Fe^{3+} aq species. *Molecular Catalysis* A: *Chemistry*, 161: 105-113.

[58] Hernandez-Alonso, M. D., Hungrıa, A. B., Martınez-Arias, A., Fernandez-Garcıa, M., Coronado, J. M., Conesa, J. C. and Soria, J. 2004. EPR study of the photoassisted formation of radicals on CeO_2 nanoparticles employed for toluene photooxidation. *Applied Catalysis* B: *Environmental*, 50 (3): 167-175.

[59] Zhai, Y. Q., Zhang, S. Y. and Pang, H. 2007. Preparation, characterization and photocatalytic activity of cerium oxide nanocrystalline using ammonium bicarbonate as precipitant. *Materials Letters*, 61: 1863-1866.

[60] Salker, A. V. and Borker, P. 2007. Solar assisted photocatalytic degradation of Naphthol Blue Black dye using $Ce_{1-x}Mn_xO_2$. *Materials chemistry and physics*, 103 (2-3): 366-370.

[61] Huang, G. F., Ma, Z. L., Huang, W. Q., Tian, Y., Jiao, C., Yang, Z. M., Wan, Z. and Pan, A. 2013. Ag_3PO_4 Semiconductor Photocatalyst: Possibilities and Challenges. *Journal of Nanomaterials*, 2013 (8): 371356.

[62] Yang, Z. M., Huang, G. F., Huang, W. Q., Wei, J. M., Yan, X. G. and Liu, Y. Y. 2014. Novel Ag_3PO_4/CeO_2 composite with high efficiency and stability for photocatalytic applications. *Journal of Materials Chemistry* A, 2: 1750-1756.

[63] Zhang, W., Hu, C., Zhai, W., Wang, Z., Sun, Y., Chi, F., Ran, S., Liu, X. and Lv, Y. 2016. Novel Ag_3PO_4/CeO_2 p-n hierarchical heterojunction with enhanced photocatalytic performance. *Materials Research*, 19 (3): 673-679.

[64] Barpuzary, D. and Qureshi, M. 2013. Enhanced photovoltaic performance of semiconductor- sensitized ZnO-CdS coupled with graphene oxide as a novel photoactive material. *ACS Applied Material Interfaces*, 5: 11673-11682.

[65] Thakur, P. and Chadha, R. 2012. Synthesis and characterization of CdS doped TiO_2 nanocrystalline powder: a spectroscopic study. *Material Research Bulletin*, 47: 1719-1724.

[66] Li, W., Xie, S., Li, M., Ouyang, X., Cui, G., Lu, X. and Tong, Y. 2013. CdS/CeOx heterostructured nanowires for photocatalytic hydrogen production. *Journal of Material Chemistry* A, 1: 4190-4193.

[67] Gu, S., Chen, Y., Yuan, X., Wang, H., Chen, X., Liu, Y., Jiang, Q., Wu, Z. and Zeng, G. 2016. Facile synthesis of CeO_2 nanoparticle sensitized CdS nanorod photocatalyst with improved visible light photocatalytic degradation of Rhodamine B. *RSC Advances*, 5: 79556-79564.

[68] You, D. T., Pan, B., Jiang, F., Zhou, Y. G. and Su, W. Y. 2016. CdS nanoparticles/CeO_2 nanorods composite with high-efficiency visible-light-driven photocatalytic activity. *Applied Surface Science*, 363: 154-160.

[69] Zhang, X., Zhang, N., Xu, Y. and Tang, Z. R. 2015. One-dimensional CdS nanowires CeO_2 nanoparticles composites with boosted photocatalytic activity. *New Journal of Chemistry*, 39: 6756-6764.

[70] Xu, A. W., Gao, Y. and Liu, H. Q. 2002. The preparation, characterization, and their photocatalytic activities of rare-earth-doped TiO_2 nanoparticles. *Journals of Catalysis*, 207: 151-157.

[71] Wang, L., Ding, J., Chai, Y., Liu, Q., Ren, J., Liu, X. and Dai, W. L. 2015. CeO_2 nanorod/g- C_3N_4/N-rGO composite: enhanced visible-light-driven photocatalytic performance and the role of N-rGO as electronic transfer media. *Dalton Transactions*, 44: 11223-11234.

[72] Wang, J., Fan, H., Chen, W., Jiao, Y., Jin, W., Zhao, Y., Zhang, S. and Yao, H. 2011. Synergistic effect of CeO_2 modified TiO_2 photocatalyst on the enhancement of visible light photocatalytic performance. *Journal of the Chinese Ceramic Society*, 39: 2002-2007.

[73] Chen, F., Ho, P., Ran, R., Chen, W., Si, Z., Wu, X., Weng, D., Huang, Z. and Lee, C. 2017. Synergistic effect of CeO_2 modified TiO_2 photocatalyst on the enhancement of visible light photocatalytic performance. *Journal of Alloys and Compounds*, doi: 10.1016/j.jallcom.2017.04.138.

[74] Chen, C., Zhao, W., Lei, P., Zhao, J. and Serpone, N. 2004. Photosensitized degradation of dyes in Polyoxometalate solutions versus TiO_2 dispersions under visible-light irradiation: mechanistic implications. *Chemical European Journals*, 10: 1956-1965.

[75] Torreshuerta, A. M., Dominguezcrespo, M. A., Brachettisibaj, S. B., Dorantesrosales, H. J., Hernandezperez, M. A. and Loiscorre, J. A. 2010. Preparation of ZnO: CeO_{2-x} thin films by AP-MOCVD: structural and optical properties. *Journal of Solid State Chemistry*, 183 (9): 2205-2217.

[76] Ma, T. Y., Yuan, Z. Y. and Cao, J. L. 2010. Hydrangea-like meso/macroporous ZnO-CeO_2 binary oxide materials: synthesis, photocatalysis and co-oxidation. *European Journal of Inorganic Chemistry*, 5: 716-724.

[77] De Lima, J. F., Martins, R. F., Neri, C R. and Serra, O. A. 2009. ZnO: CeO_2-based nanopowders with low catalytic activity as UV absorbers. *Applied Surface Science*, 255 (22): 9006- 9009.

[78] Mo, L. Y., Zheng, X. M. and Yeh, C. T. 2005. A novel CeO_2/ZnO catalyst for hydrogen production from the partial oxidation of methanol. *Chemical Physics Chemistry*, 6 (8): 1470-1472.

[79] Nidhi, H., Shah, Karan, R., Bhangaonkar, S. and Mhaske, T. 2017. In-Situ Synthesis of CeO_2/ZnO composite nanoparticles and its application in degradation of Rhodamine B using Sonocatalytic and photocatalytic method. *International Journal of Materials Science and Engineering*, 5 (1): 16-27.

[80] Rodwihok, C., Wongratanaphisan, D., Tam, T. V., Choi, W. M., Hur, S. H. and Chung, J. S. 2020. Cerium-oxide-nanoparticle-decorated zinc oxide with enhanced photocatalytic degradation of methyl orange. *Applied Science*, 10: 1697.

[81] Yuan, Y., Huang, G. F., Hu, W. Y., Xiong, DN., Zhou, B. X., Chang, S. and Huang, W. Q. 2017. Construction of g-C_3N_4/CeO_2/ZnO ternary photocatalysts with enhanced photocatalytic performance. *Journal of Physics and Chemistry of Solids*, 106: 1-9.

[82] Prabhu, S., Viswanathan, T., Jothivenkatachalam, K. and Jeganathan, K. 2014. Visible light photocatalytic activity of CeO_2-ZnO-TiO_2 composites for the degradation of Rhodamine B. *Indian Journal of Materials Science*, doi.org/10.1155/2014/536123.

[83] Pan, H., Haoxi, J. and Minhua, Z. 2012. Structures and oxygen storage capacities of CeO_2-ZrO_2- Al_2O_3 ternary oxides prepared by a green route: supercritical anti-solvent precipitation. *Journal of Rare Earths*, 30 (6): 524.

[84] Reddy, B. M., Lakshmanan, P. and Khan, A. 2004. Investigation of surface structures of dispersed V_2O_5 on CeO_2-SiO_2, CeO_2-TiO_2 and CeO_2-ZrO_2 mixed oxides by XRD, Raman, and XPS techniques. *Journal of Physical Chemistry* B, 108 (43): 16855-16863.

[85] Reddy, B. M., Khan, A., Lakshmanan, P., Aouine, M., Loridant, S. and Volta, J. C. 2005. Structural characterization of nanosized CeO_2-SiO_2, CeO_2-TiO_2, and CeO_2-ZrO_2 catalysts by XRD, Raman, and HREM techniques. *Journal of Physical Chemistry* B, 109 (8): 3355-3363.

[86] Berg, J. M., Romozer, A., Banerjee, N. and Sayes, C. M. 2009. The relationship between pH and zeta potential of 30 nm metal oxide nanoparticle suspensions relevant to in vitro toxicological evaluations. *Nanotoxicology*, 3: 276-283.

[87] Haileyesus, Tedla., Isabel, Diaz., Tesfahun, Kebede., Abi M, Taddesse. 2015. Synthesis, characterization and photocatalytic activity of zeolite supported ZnO/Fe_2O_3/MnO_2 nanocomposite. *Journal of Environmental Chemical Engineering*, 3: 1586-1591.

[88] Jin, C., Liu, G., Zu, L., Qin, Y. and Yang, J. 2015. Preparation of Ag/Ag_3PO_4/ZnO ternary heterostructured for photocatalytic studies. *Journal of Colloid and Interface Science*, 453: 36-41.

[89] Lee, K., Cho, S., Park, S. H., Heeger, A. J., Lee, C. W. and Lee, S. H. 2006. Metallic transport in polyaniline. *Nature*, 441 (7089): 65-68.

[90] Bu, Y. and Chen, Z. 2014. Role of polyaniline on the photocatalytic degradation and stability performance of the Polyaniline/Silver/Silver Phosphate composite under visible light. *American Chemical Society of Applied Material Interfaces*, 6 (20): 17589-17598.

[91] Zhang, H., Zong, R., Zhao, J. and Zhu, Y. 2008. Dramatic visible photocatalytic degradation performances due to synergetic effect of TiO_2 with PANI. *Environmental Science Technology*, 42 (10): 3803-3807.

[92] Ge, L., Han, C. and Liu, J. 2012. In situ synthesis and enhanced visible light photocatalytic activities of novel PANI/g-C_3N_4 composite photocatalysts. *Journal of Material Chemistry*, 22 (23): 11843-11850.

[93] Zhang, L. J. and Wan, M X. 2003. Polyaniline/TiO_2 nanocomposite nanotubes. *Journal of Physical Chemistry*, 107 (28): 6748-6753.

[94] Fujishima, A., Rao, T. N. and Tryk, D. K. 2000. Titanium dioxide photocatalysis. *Journal of Photochemistry and Photobiology* C: *Photochemistry Reviews*, 1 (1): 1-21.

[95] Hidalgo, D., Bocchini, S., Fontana, M., Saraccob, G. and Hernandez, S. 2015. Green and low- cost synthesis of PANI-TiO_2 nanocomposite mesoporous films for photoelectrochemical water splitting. *Royal Society of Chemistry*, 5: 49429-49438.

[96] Ameen, A., Akhtar, M. S., Kim, Y. S., Yang, B. and Shin, H. S. 2011. An effective nanocomposite of polyaniline and ZnO: preparation, characterizations, and its photocatalytic activity. *Colloid Polymer Sciences*, 289: 415-421.

[97] Li, J., Zhu, L., Wu, Y., Harima, Y., Zhang, A. and Tang, H. 2006. Green and low-cost synthesis of PANI/TiO_2 nanocomposite mesoporous films for photoelectrochemical water splitting. *Polymer*, 47: 7361-7367.